Iranian Journal of Energy & Environment
Journal Homepage: www.ijee.net
IJEE an official peer review journal of Babol Noshirvani University of Technology, ISSN:2079-2115

An Axial Hydro-Kinetic Turbine for Optimum Power Extraction Using Tidal Dams

A. Zahedi Nejad*[1] and P. Zahedi Nejad[2]

[a] *Department of Mechanical and Aerospace Engineering, Science and Research Branch, Islamic Azad University, Tehran, Iran*
[b] *Department of Mechanical Engineering, Shiraz Branch, Islamic Azad University, Shiraz, Iran*

P A P E R I N F O

Paper history:
Received 11 January 2018
Accepted in revised form 10 March 2018

Keywords:
Energy resource
Power-coefficient
Renewable energy
Shape optimization
Tidal turbine

A B S T R A C T

The present paper describes analytical optimization and numerical simulation of a modern hydro-kinetic turbine. It was a tidal turbine with twin elliptic-rotors. The turbines were installed within the twin ducts inside of a tidal dam. There was a gap between each of the turbines and the ducts for allowing vortex formation around each of turbines. The pitch angle distribution was optimized for highest energy extraction from water flow. The numerical simulations of the turbine have shown great power-coefficient that exceeds from 1.0 for tip-speed ratios greater than 3.5. According to power-coefficient curve, the runaway speed for the hydro-kinetic turbine was eliminated and the extracted power has increased with a second order function at higher tip-speed ratios. Based on obtained data, an axial hydro-kinetic turbine can not only absorb flow kinetic energy of incoming flow, but also can extract energy from parallel flows over each turbine. The power-coefficient curve against tip-speed ratio encounters with a break point around tip-speed ratio of 3.0. Simultaneously a strong vortex ring has formed around each of turbines. Flow trajectories illustrate how the hydro-kinetic turbine was able to absorb much more energy from external flows than conventional axial hydro-kinetic turbines.

***doi**: 10.5829/ijee.2018.09.01.10*

NOMENCLATURE

a_0	Calibration constant
C_P	Power-coefficient of the turbine
C_D	Drag coefficient of the turbine
$\dot{E}$	Extracted power
f	Distribution function for blade position over spherical surface
$\dot{m}$	Mass flow rate over turbine blades
N	Number of frontal blades of the turbine
R	Radius of sphere
R_0	smaller radius of elliptic hub
T	Holding torque of the turbine
U	Flow velocity over spherical surface
V	Flow velocity in narrow channels of turbine
X	X-coordinate
Y	Y-coordinate
Greek Symbols	
α_0	Ideal angle of attack
β	Flow angle over spherical surface
λ	Local tip-speed ratio
λ_0	Tip-speed ratio based on radius of sphere
θ	Pitch angle
θ_i	Inflow angle
θ_e	Outflow angle
ω	Angular speed of the turbine
λ_0	Tip-speed ratio based on radius of sphere
θ	Pitch angle
Subscripts	
e	Exit from blade
i	Inter to blade
j	Blade row number
opt	Optimum value
∞	Free stream flow

INTRODUCTION

During past decades energy absorption from river flows and tidal currents has been commercialized in many countries [1]. A hydro-kinetic turbine extracts energy from kinetic energy of water flow. The minimum required mean flow velocity for employing hydro-kinetic

* Corresponding author: Ali Zahedi Nejad
E-mail: ali.zahedinejad@srbiau.ac.ir

turbines in rivers is between 1.0 to 1.5 m/s [2]. Tidal turbines are related technology to river turbines but they extract energy from sea or ocean currents. In early 1990s, various types of tidal and river turbines were built. Innovative designs in the United States and United Kingdom, led to construct small hydro-turbines with names Stingray and Sea-Snail and gained significant public attention [2]. Setuguchi et al. [1] designed and manufactured a diffuser-enhanced duct with two passages. They introduced duct shape as a key factor for increasing the efficiency of a hydro-kinetic turbine [1]. Garrett et al. [3] studied maximum attainable energy by a fence of axial flow turbines. Munch et al. [4] investigated numerically a four blade ducted tidal turbine. They simulated numerically transient turbulent flow in ANSYS CFX software. They showed that with tip-speed ratio of seven, the turbine power-coefficient exceeds 55% [4]. Yaakob et al. [5] had designed and tested a Savonius vertical axis turbine for absorbing kinetic energy from very low speed (0.56 m/s) tidal flows [6]. ANSYS-CFX software was used to find overall efficiency of a diffuser enhanced tidal turbine. Also, velocity decay for collinear axial hydro-kinetic turbines was studied Wake flow of a two-rotor hydro-kinetic turbine was investigated. Mehmood et al. [8] studied many diffuser designs for tidal current turbines. Schileicher et al. [9] numerically designed and simulated a rotor of a hydro-kinetic turbine for the highest energy extraction from water flow. Ziaei et al. [10] described manufacturing process of a micro-turbine. They employed CNC machining for manufacturing a prototype of microturbine. A conceptual design for duct shape for horizontal axis hydro-kinetic turbines was introduced and extensive duct shapes were numerically studied [11]. The optimum duct shape had the greatest frictional drag coefficient and the minimum flow separation [11]. Zahedi Nejad and Rad demonstrated an analytical model for instantaneous energy exchange during rigid interaction of rotor with unsteady water flow around duct of axial tidal turbines [12]. Zahedi Nejad et al. [13] defined the method of design and manufacturing of a multi-diffuser axial hydro-kinetic turbine. They have manufactured a ducted hydro-kinetic turbine comprised of two high performance propellers with a duct that could convert to many experimental models for investigation of various diffuser enhancing effects [13]. All steps of design, fabrication and test of an axial turbine were described in literature [14]. The power-coefficient of the invented turbine was gradually increased with increasing turbine's dimensions without changing geometric parameters [14]. The present paper introduces an innovative design for hydro-kinetic turbines. Fig. 1 illustrates the twin tidal turbines inside ducts of a tidal dam. The throat diameters of the ducts are 40 percent greater than the diameter of hydro-kinetic turbines. Two generators were installed directly to each of the twin hydro-kinetic turbines. The sluice gate was designed for controlling water flow when level differences of sea water makes powerful currents through ducts. The introduced turbine in Figs. 1 and 2 is a modern and an efficient design of tidal turbine.

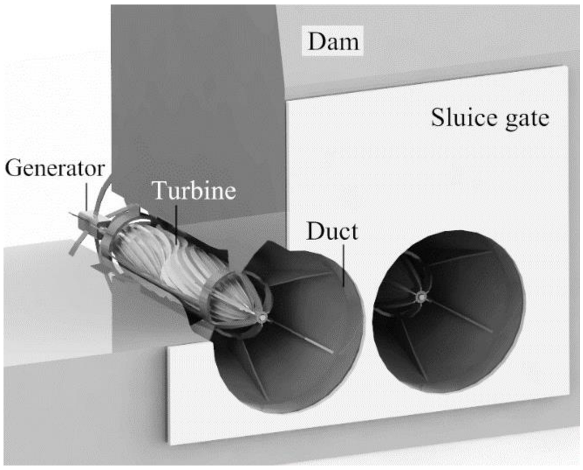

Figure 1. The twin turbines inside ducts of a tidal dam.

The top-view of the tidal dam with twin turbines is shown in Fig. 2. The frontal and rear supports hold the turbines within the ducts. The two turbines are parallel but have blades in reverse directions to hold symmetric flow condition. The top-view of the sluice gate was also demonstrated.

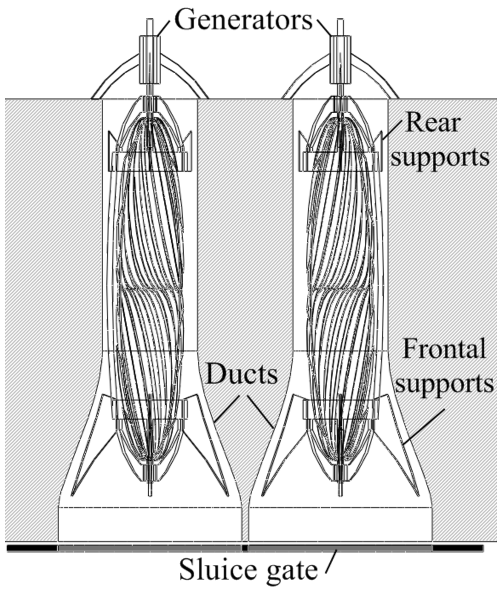

Figure 2. Top view of the twin tidal turbine located inside of the dam. A section view of the dam was shown for better illustration.

Analytical derivations for designing elliptic hydro-kinetic turbines

In present paper, optimum pitch angle θ_{opt} was calculated by equation 1 [12].

$$\theta_{opt} = \tan^{-1}(\lambda) + \alpha_0 \quad (1)$$

As illustrated in Fig. 3, considering potential flow over a sphere, the local tip-speed ratio becomes a function of Y-coordinate:

$$\lambda = r_{(Y)}\,\omega / U_{(Y)} \quad (2)$$

The optimum slope of Y=f(X) curve in Fig. 3-a, is

$$\begin{aligned}(dY/dX)_{opt} &= \tan(\theta_{opt} - \alpha_0) \\ &= \lambda_{opt} = \left(r_{(Y)}\,\omega / U_{(Y)}\right)_{opt}\end{aligned} \quad (3)$$

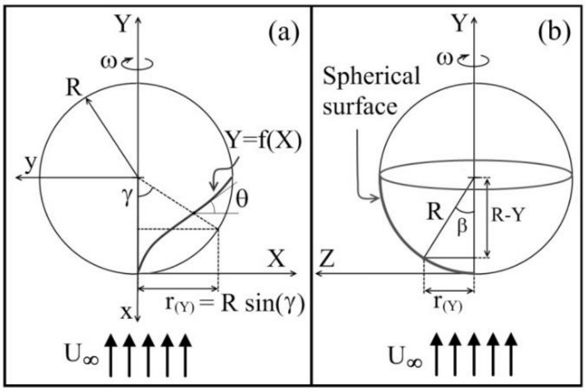

Fig. 3: a) Top view of spherical hub. The turbine rotates around x-axis. b) Side view of spherical hub. The potential flow was considered around the stationary sphere.

Considering potential flow over spherical hub as shown in Fig. 3-b the function $U_{(Y)}$ is analytically approximated. The potential flow theory for uniform flow over spherical surface of the hub yields:

$$U_{(Y)} = U_{(\beta)} = \frac{3}{2} U_\infty \sin(\beta) \quad (4)$$

According to this figure the trigonometric relations in Eq. (5) were obtained:

$$R\sin(\beta) = r(Y),\ R\cos(\beta) = R - Y \quad (5)$$

From trigonometric relations and Eq. (5) the $\sin(\beta)$ is written as a function of Y-coordinate:

$$\sin(\beta) = \sqrt{2(Y/R) - (Y/R)^2} \quad (6)$$

Inserting $\sin(\beta)$ from Eq. (6) in the Eq. (4) yields the flow velocity over spherical surface.

$$U_{(Y)} = \frac{3}{2} U_\infty \sqrt{2(Y/R) - (Y/R)^2} \quad (7)$$

Combining Eq. (3) with Eqs. (4-7) yields the optimum distribution for slope function df/dX:

$$\begin{aligned}(dY/dX)_{opt} &= \left(r_{(Y)}\,\omega / U_{(Y)}\right)_{opt} \\ &= \frac{\left(R\sqrt{2(Y/R) - (Y/R)^2}\right)\omega}{\left(\frac{3}{2} U_\infty \sqrt{2(Y/R) - (Y/R)^2}\right)} \\ &= \frac{2}{3}\frac{R\omega}{U_\infty} = \frac{2}{3}\lambda_0\end{aligned} \quad (8)$$

Integration from optimum slope distribution in eq. (8) yields the function f(X) :

$$\begin{aligned}Y = f(X) &= \int (dY/dX)_{opt}\, dX \\ &= \int \frac{2}{3}\frac{R\omega}{U_\infty} dX = \left(\frac{2}{3}\frac{R\omega}{U_\infty}\right) X = \left(\frac{2}{3}\lambda\right) X\end{aligned} \quad (9)$$

Based on Eq. (9), the function f(X) is a linear function with zero abscissa and constant slope. Considering potential flow, the function f(X) is also a linear function for backward blades. While the derivations were presented for a spherical hub, a similar linear function is also valid for elliptic hub that has been shown in Fig. 4.

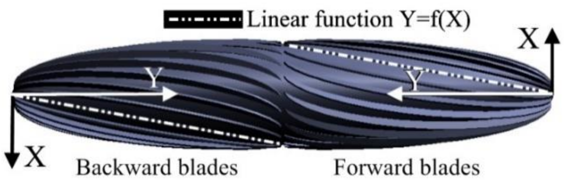

Fig. 4: Linear function f(X) with zero abscissa for forward and backward blades.

Analytical derivation of power-coefficient as a function of tip-speed ratio

Considering Fig. 5, for each blade to blade spacing with subscript j the fluid mass flow rate $\dot{m}_j$ exerts a torque T_j on the turbine. The torque is expressed as Eq. (10):

$$T_j = \dot{m}_j\left(\vec{V}_e \times \vec{R}_e - \vec{V}_i \times \vec{R}_i\right)_j \quad (10)$$

For each blade with subscript j the extracted power $\dot{E}_j$ is written as:

$$\dot{E}_j = T_j\omega = \dot{m}_j\left(V_e R_e \sin\theta_e - V_i R_i \sin\theta_i\right)\omega \quad (11)$$

The mass flow rate through each blade row is a portion of total mass flow rate over the turbine. For blade row number j the mass flow rate with subscript j is:

$$\dot{m}_j = \frac{\dot{m}}{N} = \pi\rho U_\infty R_0^2 / N \quad (12)$$

The parameter N in Eq. (12) is the number of frontal blades for elliptic turbine. According to Fig. (5), the following values are found:

$$\begin{aligned} &R_e = R_0, R_i = 0, \theta_i = 0 \\ &\sin\theta_e = R_0\omega / \sqrt{\left(\dot{m}_j / \rho (A_e)_j\right)^2 + (R_0\omega)^2} \\ &(V_e)_j = \sqrt{\left(\dot{m}_j / \rho (A_e)_j\right)^2 + (R_0\omega)^2} \end{aligned} \quad (13)$$

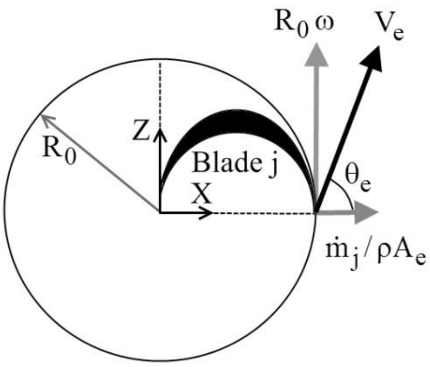

Fig. 5: Turbo-machine parameters for deriving power-coefficient as a function of tip-speed ratio.

Replacing values of Eqs. (12) and (13) in Eq. (11) yields:

$$\begin{aligned} \dot{E} &= \sum_{1}^{2N} \dot{E}_j \\ &= 2N\dot{m}_j\left(V_e R_e \sin\theta_e - V_i R_i \sin\theta_i\right)_j \omega \\ &= 2\pi\rho U_\infty R_0^4 \omega^2 \end{aligned} \quad (14)$$

The power-coefficient of the turbine is calculated by Eq. (15).

$$\begin{aligned} C_P &= \frac{\dot{E}}{0.5\rho U_\infty^3 A_0} = \frac{2\pi\rho U_\infty R_0^4 \omega^2}{0.5\rho U_\infty^3 \pi R_0^2} \\ &= 4\left(\frac{R_0\omega}{U_\infty}\right)^2 = 4\lambda_0^2 \end{aligned} \quad (15)$$

CFD simulation results and discussion

SolidWorks Flow-Simulation software was used for modeling water flow with cavitation around the tidal turbine. The solution parameters and governing equations were discussed in literature [11]. The minimum velocity of water current required according to the literature is typically in the range of 1.03 to 2.06 m/s [15]. Optimum currents are in the range of 2.57 to 3.6 m/s [15]. In present paper the simulations were performed for optimum currents of 3.0 m/s which was also reported in literature [11, 15]. Many numerical simulations were carried out by illustration of the performance of the elliptic turbine in water flow with uniform velocity of 3 m/s. A model turbine with small scale was designed and the CFD simulations performed for the model. The smallest radius of elliptic turbine (0.05 m) and its length of 0.5 m resulted in the flow velocity of m/s and the Reynolds number of 2.9×10^5.

The power-coefficient of the hydro-kinetic turbine for the flow velocity of 3 m/s is plotted in Fig. 6. There is a break point in the curve of power-coefficient after tip-speed ratio of 3.0. For higher values of tip-speed ratio a vortex ring is generated around the turbine as shown in Fig. 8. The power-coefficient of the hydro-kinetic turbine increases with a second-order function after tip-speed ratio of 3.0. There is no upper limit for power-coefficient of the introduced hydro-kinetic turbine at high tip-speed ratios. The increase of power coefficient is originated from exchange and circulation of low and high pressure flows around elliptic turbine.

As shown in Fig. 6 the power-coefficient curve has a parabolic growth after $\lambda_0 = 3.0$.

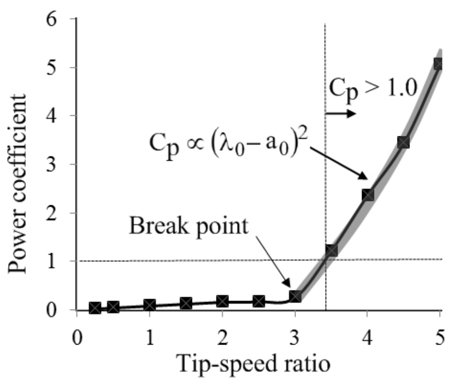

Fig. 6: Power-coefficient against tip-speed ratio for uniform flow of water with speed 3 m/sec in the axial direction.

An approximate value for power-coefficient is $C_P \propto (\lambda_0 - a_0)^2$ in which a_0 is a calibration constant. The parabolic curve in Fig. 6 well reads analytical derivations (Eq. (15)) for power-coefficient as a function of tip-speed ratio.

Fig. 7 illustrates the curve of drag force coefficient against tip-speed ratio. The drag force coefficient increases with tip-speed ratio. It encounters with a break point at the tip-speed ratio of 3.0. Comparison of Figs. 6 and 7 illustrate that the drag force coefficient increases with increase of power-coefficient.

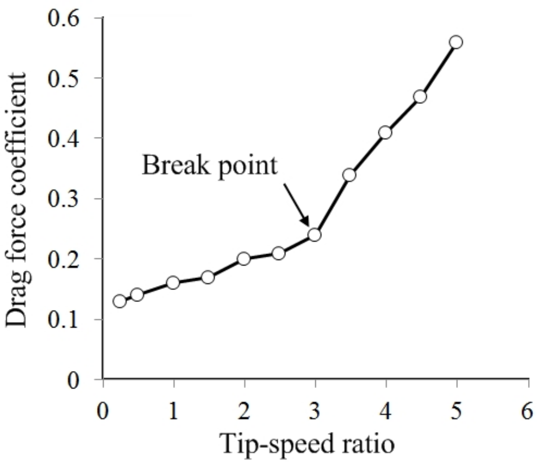

Fig. 7: Drag coefficient against tip-speed ratio for uniform flow of water with speed 3 m/sec in the axial direction.

Flow trajectories over a blade of the hydro-kinetic turbine were plotted for illustrating flow paths during energy extraction. As shown in Fig. 8, a vortex ring is formed at the middle portion of the turbine. The middle portion of the turbine exchanges high pressure flow with low pressure flow. The tip-speed ratio for the graph in this figure is 5.0.

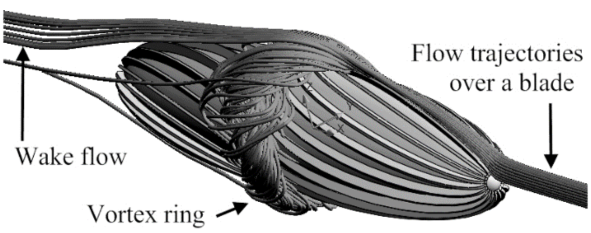

Fig. 8: Flow trajectories over a blade of the turbine in water with uniform speed of 3.0 m/sec in the axial direction.

The total pressure refers to the sum of static pressure, dynamic pressure, and gravitational head, as expressed by Bernoulli's principle. Fig. 9 illustrates contours of total pressure on a cut plane from top view. The tip-speed ratio is 5.0. The angular speed of the turbine is 300 rad/s. The symmetry boundary condition was defined for external flow boundaries. The difference in water level (0.7 m) on two sides of the tidal dam makes difference in total pressures on two sides of the tidal dam. The total pressure distribution in Fig. 9 indicates how the twin turbines absorb fluid energy and reduce the total pressure. In this simulation, the average flow speed in front of the dam was 0.1 m/s, the flow velocity in the ducts is 3.0 m/s and both turbines diameters were 0.1 m.

Fig. 9: Total pressure distribution for uniform flow of water with speed of 1 m/sec in the axial direction. The turbine rotation speed is 300 rad/sec.

CONCLUSION

The present paper introduced design of a modern hydro-kinetic turbine for optimum power extraction using tidal dams. The main concluding remarks of this work are listed below.

- The optimum blade shape for an elliptic turbine is a planar surface with orientation that construct linear function Y=f(X) on the surface of the elliptic hub.
- The backward blades over elliptic hub of the axial hydro-kinetic turbine can significantly increase power-coefficient of the hydro-kinetic turbine.
- Based on numerical and analytical investigations in this work, an axial hydro-kinetic turbine can not only absorb flow kinetic energy of the incoming flow, but-also can extract energy from parallel flows over

the turbine. The recovery of fluid total-pressure with fluid circulation at the middle portion of the turbine provides additional energy for absorption by the turbine. This energy recovery yields power-coefficients that can highly exceed from 1.0.

- Flow trajectories for $\lambda > 3.0$ explain how power-coefficient of the hydro-kinetic turbine can exceed without bound while a vortex ring is observed based on the numerical simulations.
- The total pressure recovery exists in the flow around hydro-kinetic turbine. This is an Innovative design of axial hydro-kinetic turbine with power-coefficient that exceeds 1.0.
- Having power-coefficients greater than 1.0 is meaningful: 'The optimized hydro-kinetic turbines can extract much more power than conventional axial turbines'.
- The power-coefficient curve against tip-speed ratio for hydro-kinetic turbine has no upper limit. It doesn't have a runaway speed. This means the hydro-kinetic turbine can extract high values of power from external flow at very high tip-speed ratios.

REFERENCES

1. Setoguchi T., Shiomi N., Kaneko K., 2004, "Development of two-way diffuser for fluid energy conversion system". Renewable Energy, Vol. 29, No 10, 1757 - 1771.
2. Ginter, V. and Bear, C., 2007, "Development and application of a water current turbine", New Energy Corporation Inc., 1-14.
3. Garrett C., Cummins P., 2008, "Limits to tidal current power". Renewable Energy, Vol. 33, No 11, 2485 - 2490.
4. Munch, C., Vonlanthen, M., Gomes, J., Luquet, R., Guinard, P., Avellan, F., 2009, "Design and Performance Assessment of A Tidal Ducted Turbine", In Proceedings of the 3rd IAHR International Meeting of the Workgroup on Cavitation and Dynamic Problems in Hydraulic Machinery and Systems., Brno, Czech Republic., 571–581.
5. Yaakob O. B., Tawi K.B., 2010, Suprayogi Sunanto D.T., "Computer simulation studies on the effect overlap ratio for savonius type vertical axis marine current turbine". International journal of engineering (IJE), Transactions A: Basics, Vol. 23, No. 1, 79-88.
6. Yaakob O. B., Suprayogi D., Abdul Ghani M., Tawi K., 2013, "Experimental studies on savonius-type vertical axis turbine for low marine current velocity", International journal of engineering (IJE), Transactions A: Basics, Vol. 26, No. 1, 91-98.
7. K. Wern, W. H. Lam, K.C. Ching, 2013, "Review 2002-2012: 10 years research progress in horizontal-axis marine current turbines", Open access energies, Vol. 6, 1497-1526.
8. Mehmood N., Liang Z., Khan J., 2012, "study of NACA 0015 for diffuser design in tidal current turbine applications". Technical note, International journal of engineering (IJE), Transactions C: Aspects, Vol. 25, No. 4, 373-380.
9. Schleicher, W. C., Riglin, J. D., Kraybill, Z. A., Oztekin, A., 2013, "Design and simulation of a micro hydrokinetic turbine". Proceedings of the 1st Marine Energy Technology Symposium, METS13, Washington, D.C; 1 .
10. Ziaei Tabatabaei S. S., Hashemi A., Zolghadr shojai A., Meysami A., 2015, "The manufacturing process of a 100-kw prototype microturbine as a distributed generation method in iran". Technical note, International journal of engineering (IJE), Transactions A: Basics, Vol. 28, No. 1, 145 - 153.
11. Zahedi Nejad A., Rad M., Khayyat M., 2016, "Conceptual duct shape design for horizontal axis hydro-kinetic turbines". Scientia Iranica; International Journal of Science and Technology. Transactions B: Mechanical engineering. Vol. 3, No 25, 2113 - 2124.
12. Zahedi Nejad A., Rad M., 2017, "Modeling instantaneous energy exchange during rigid interaction of rotor with unsteady water flow around duct of axial tidal turbines", Modaress Mechanical Engineering, Vol.16, No 12, 692-702 (in Persian).
13. Zahedi Nejad A., Rad M., Khayyat M., 2017, "Numerical and experimental investigation for design of a high performance micro hydro-kinetic turbine". International journal of engineering (IJE). Transactions B: Application. Vol 30, No 5, 785-790.
14. Rad, M., Zahedi Nejad, A., 2017, "Fabrication and test of an axial wind turbine with the most power during absorbing flow kinetic energy". Amirkabir journal of mechanical engineering. Article in press, , (DOI): 10.22060/MEJ.2017.12269.5299.
15. Ladokun, L.L., Ajao, K.R. and Sule, B.F., 2013, "Hydro-kinetic energy conversion systems: prospects and challenges in Nigerian hydrological setting", Nigerian Journal of Technology, Vol. 32, No 3, 538-549.

Persian Abstract

DOI: 10.5829/ijee.2018.09.01.10

چکیده

مقاله حاضر بهینه سازی تحلیلی و شبیه سازی عددی یک توربین انرژی-جنبشی جدید را شرح می دهد. این یک توربین جزر و مدی با روتور بیضوی دو قلو است. توربین ها درون داکتهای دو قلو در داخل یک سد جزر و مدی نصب شدند. یک فاصله بین هر یک از توربین ها و داکت ها وجود دارد تا اجازه تشکیل گردابه در اطراف هر یک از توربین ها داده شود. برای بیشترین استخراج انرژی از جریان آب توزیع زاویه گام بهینه سازی شده است. شبیه سازی های عددی توربین ضریب توان بزرگی را نشان داده اند که برای نسبت سرعت نوک بالاتر از ۳/۵ بالاتر از ۱/۰ است. مطابق منحنی ضریب توان سرعت دوران آزاد توربین انرژی-جنبشی حذف می شود و در نسب های سرعت نوک بزرگتر، توان استخراج شده با تابع درجه دو افزایش می یابد. بر اساس بررسی های انجام شده در مقاله حاضر یک توربین انرژی-جنبشی محوری نه تنها قادر است انرژی جنبشی جریان ورودی را جذب کند بلکه توانایی جذب انرژی از جریان های موازی هر یک از توربین ها را دارد. منحنی ضریب توان در مقابل نسبت سرعت نوک با یک نقطه شکست در اطراف نسبت سرعت نوک ۳/۰ مواجه است. به صورت همزمان یک حلقه گردابه ای قوی در اطراف هر یک از توربین ها تشکیل می شود. خطوط مسیر جریان مشخص می کند که چگونه توربین انرژی-جنبشی قادر است در مقایسه با توربین های انرژی-جنبشی رایج انرژی بیشتری را از جریان های خارجی جذب کند.